Materials Research Bulletin 47 (2012) 3473–3478

Contents lists available at SciVerse ScienceDirect

Materials Research Bulletin

journal homepage: www.elsevier.com/locate/matresbu

Phosphotungstic acid supported on magnetic nanoparticles as an efficient reusable catalyst for epoxidation of alkenes

M. Kooti [*], M. Afshari

Department of Chemistry, College of Science, Shahid Chamran University, Ahvaz 61357- 43169, Iran

ARTICLE INFO

Article history:
Received 13 March 2012
Received in revised form 26 June 2012
Accepted 4 July 2012
Available online 13 July 2012

Keywords:
A. Nanostructures
A. Magnetic materials
A. Composites
D. Catalytic properties

ABSTRACT

A new magnetically separable catalyst consisting of phosphotungstic acid supported on imidazole functionalized silica coated cobalt ferrite nanoparticles was prepared. The synthesized catalyst was characterized by X-ray powder diffraction (XRD), transmission electron microscopy (TEM), vibrating sample magnetometry (VSM), thermogravimetric analysis (TGA), Fourier transform infrared (FT-IR), and inductively coupled plasma atomic emission spectroscopy (ICP-AES). This immobilized phosphotungstic acid was shown to be an efficient heterogeneous catalyst for the epoxidation of various alkenes using tert-butylhydroperoxide (*t*-BuOOH) as oxidant. The catalyst is readily recovered by simple magnetic decantation and can be recycled several times with no significant loss of catalytic activity.

1. Introduction

Epoxidation of alkenes is an important reaction due to the wide applications of epoxides in the production of various valuable materials [1]. So far, many transition metal compounds have been used as catalyst in the transformation of alkenes to epoxides. Among them polyoxometalates (POMs), an immense class of oxygen bridged metal cluster anions of mainly tungsten(VI) and molybdenum(VI), are known as highly efficient green catalysts for epoxidation reactions [2–4]. Despite of some advantages, there exist a number of drawbacks about catalysis with POMs based systems, such as high solubility in polar solvents and low surface area. Therefore, in a homogeneous reaction the isolation of the products and reuse of the catalyst become difficult. One of the most promising solutions to these problems seems to be immobilization of POMs onto solid support such as silica [5], zeolite [6], and alumina [7]. While supporting of POMs on solid materials can greatly enhance the catalytic activity, this approach still could not avoid the separation difficulty of catalyst from solution media. Therefore, further development of the catalytic system will require advanced materials that can efficiently catalyze chemical reactions and be recycled through simple separation processes.

Magnetic nanoparticles (MNPs) have recently emerged as attractive materials either as catalysts or support for immobilization of homogeneous catalysts [8–10].

The main advantage of a catalytic system based on magnetic nanoparticles is that the nanoparticles can be efficiently isolated from the product solution through a simple magnetic separation process after completing the reactions. Therefore, catalytic systems developed on MNPs supports have been successfully used in catalyzing a wide range of organic reactions including C–C coupling [11], hydrogenation [12], oxidation [13] and polymerization [14]. The catalytic systems devised by employing superparamagnetic nanoparticles as a support and their performance in catalyzing various organic reactions have been recently discussed in two excellent reviews [15,16].

Among various MNPs, $CoFe_2O_4$ has gained extensive attention due to its prominent chemical stability and other interesting properties [17–19]. However, cobalt ferrite and other MNPs tend to aggregate in liquid media due to their magnetic dipole–dipole interaction. This will lead to the reduction of their surface area and partial loss of magnetism. Therefore, some strategies have been used to chemically stabilize the naked MNPs and prevent their agglomeration in solutions, such as encapsulation them with polymers [20,21] or hydroxyapatite [22] and coating with a thin layer of silica. Silica has been considered to be one of the most ideal materials for coating of MNPs due to its characteristic including high chemical stability, biocompatibility, and easy functionalization [23–25].

There are many reports on the preparation and applications of silica coated magnetic nanoparticles [26–28]. However, to the best of our knowledge, only a few reports were devoted to the grafting of POMs on MNPs supports [29–31]. In the present work, a novel method for immobilization of phosphotungstic acid (PTA) on imidazole-functionalized silica coated cobalt ferrite nanoparticles

---

[*] Corresponding author. Tel.: +98 916 1115451; fax: +98 611 3331042.
E-mail address: m_kooti@scu.ac.ir (M. Kooti).

0025-5408/$ – see front matter © 2012 Elsevier Ltd. All rights reserved.
http://dx.doi.org/10.1016/j.materresbull.2012.07.001

is reported. The prepared composite was successfully used as catalyst toward epoxidation of some alkenes in the presence of *t*-BuOOH.

2. Experimental

2.1. General

All chemicals were purchased from Sigma–Aldrich or Merck and used as received. Phosphotungstic acid (PTA) was synthesized according to the previously reported method [32]. X-ray diffraction (XRD) patterns were recorded with a Philips X-ray diffractometer (Model PW1840). FT-IR spectra were obtained using BOMEM MB-Series 1998 FT-IR spectrometer. Magnetic properties of all the studied MNPs were measured with a vibrating sample magnetometer (VSM), Meghnatis Daghigh Kavir Company at room temperature. GC experiments were performed with a Shimadzu GC-16A instrument using a 2 m column packed with silicon DC-200 or Carbowax 20 m. ^{1}H NMR spectra of the epoxidation products were recorded in $CDCl_3$ on a Bruker Advanced DPX 400 MHz spectrometer.

2.2. Synthesis of phosphotungstic acid immobilized on imidazole functionalized Si–MNPs

Cobalt ferrite MNPs were prepared using the procedure reported by Maaz et al. [33]. Silica coated $CoFe_2O_4$ nanoparticles (Si–MNPs) were made by using sol–gel method [34]. A schematic representation for the synthesis of PTA anchored on imidazole functionalized silica coated cobalt ferrite nanoparticles is shown in Scheme 1. In the first step, a mixture of 3-chloromethoxypropylsilane (4.4 mL, 24 mmol) and imidazole (1.63 g, 24 mmol) was heated at 110 °C for 24 h with continuous stirring under N_2 atmosphere. The product (Si–imid) of this step was dissolved in 25 mL of ethanol. After addition of Si–MNPs (0.75 g) to the ethanolic solution, the mixture was refluxed for 24 h. The produced imidazole functionalized silica coated magnetic nanoparticles (Si–imid@ Si–MNPs) were magnetically separated and washed twice with ethanol and ether. Finally, Si–imid@ Si–MNPs were dispersed into 30 mL of acetonitrile, PTA (1.56 g, 0.54 mmol) was added to this solution and the whole mixture was refluxed overnight. After that, the expected final product, PTA/Si–imid@ Si–MNPs, was separated by magnetic decantation and washed with acetonitrile and dichloromethane and left to dry in a desiccator.

2.3. Catalytic studies

In a typical run, a 25 mL round-bottom flask equipped with a condenser and magnetic stirrer, was charged with: PTA/Si–imid@ Si–MNPs catalyst (0.1 g), 1,2-dichloroethane (5 mL), alkene (1 mmol), and *t*-BuOOH (2 mmol). This mixture was heated in an oil bath at 70 °C and the progress of the reaction was monitored by GC. At the end of the reaction, CH_2Cl_2 was added to dilute the reaction mixture and the organic layer was simply decanted by means of an external magnet. The decanted solution was purified on a silica-gel plate or a silica-gel column to obtain the pure product. The identities of the products were confirmed by FT-IR and ^{1}H NMR spectral data.

3. Results and discussion

3.1. Characterization of phosphotungstic acid supported on imidazole silica-coated cobalt ferrite

Immobilization of PTA on imidazole functionalized MNPs combines the advantages of ionic liquids with those of heterogeneous catalysts [35]. The as-prepared ionic liquid-modified supported catalyst provides a hydrophobic environment for organic reactions, as reported by other research groups [36–38]. The PTA moiety is bonded strongly to Si–imid@ Si–MNPs by means of ionic interaction which prevents/reduces leaching of the catalyst in polar solvents [39]. The PTA/Si–imid@ Si–MNPs catalyst was synthesized by a multi-step procedure, as shown in Scheme 1, and characterized by various techniques.

The FT-IR spectrum of MNPs (Fig. 1A) shows the expected Fe–O stretching absorption at 577 cm^{-1} which shifts to high wave numbers of 588.9 cm^{-1} after coating with silica [40]. Two new bands at 1088 cm^{-1} and 802 cm^{-1} were observed which are ascribed to the symmetrical and asymmetrical vibrations of the Si–O–Si bonds [41]. The FT-IR spectrum of PTA/Si–imid@ Si–MNPs

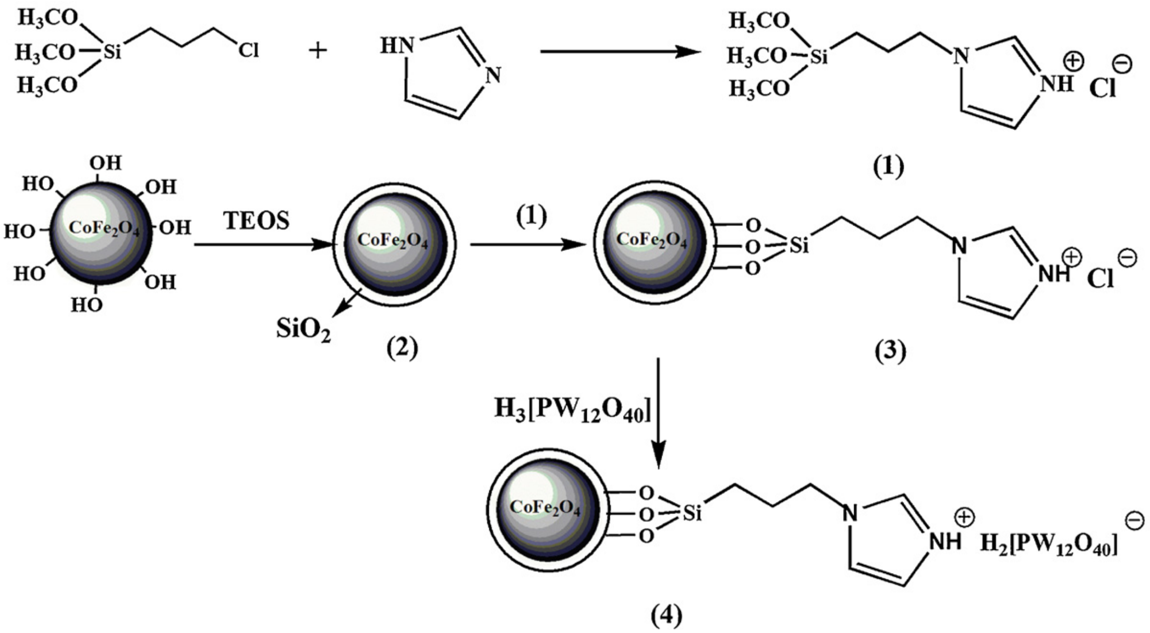

Scheme 1. Schematic representation of the formation of PTA/Si–imid@ Si–MNPs catalyst.

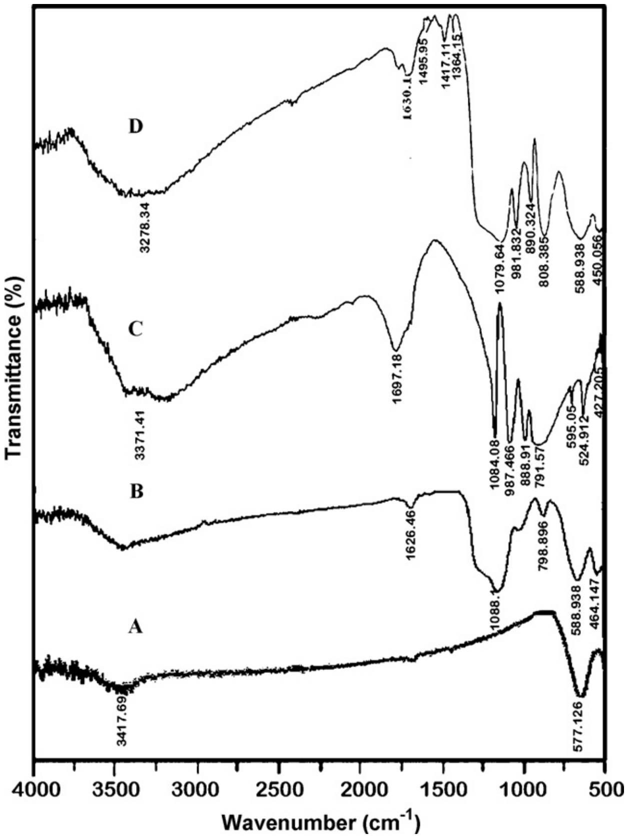

Fig. 1. FT-IR spectra of (A) MNPs, (B) Si–MNPs, (C) neat PTA and (D) PTA/Si–imid@ Si–MNPs.

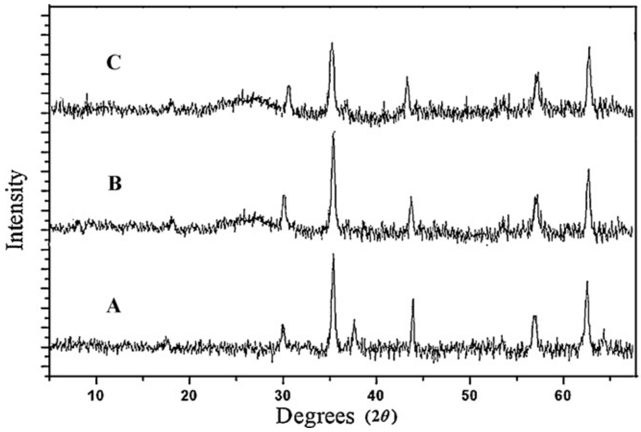

Fig. 2. XRD pattern of (A) MNPs, (B) Si–MNPs and (C) PTA/Si–imid@ Si–MNPs.

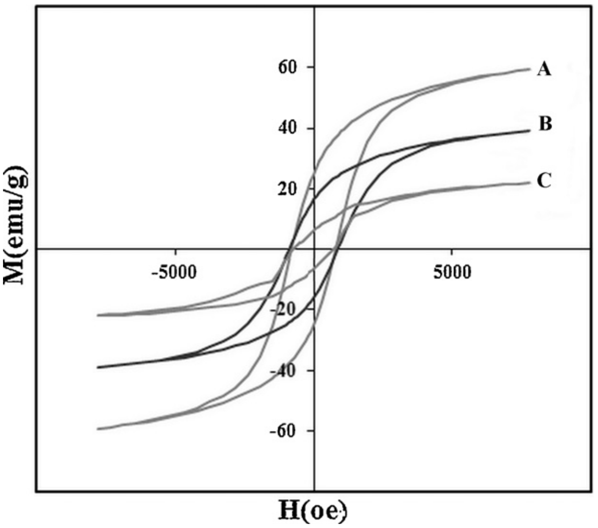

Fig. 4. Hysteresis loops of (A) MNPs, (B) Si–MNPs and (C) PTA/Si–imid@ Si–MNPs.

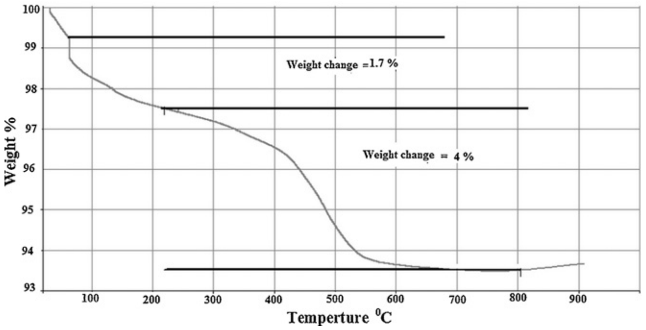

Fig. 5. TGA of PTA/Si–imid@ Si–MNPs.

(Fig. 1D) shows weak peaks in the range between 1400 and 1630 cm^{-1} assigned to the imidazole ring [42]. Two other bands at 890 cm^{-1} and 981 cm^{-1} are also observed in this spectrum, which are respectively attributed to W–O–W and W═O stretching modes of PTA [39,42].

The X-ray diffraction patterns of MNPs, Si–MNPs and PTA/Si–imid@ Si–MNPs are shown in Fig. 2.The peaks are compatible with pure $CoFe_2O_4$ phase (JCPDS PDF #221086), indicating the retention of cubic reverse spinel structure of $CoFe_2O_4$ after coating and functionalization. A weak broad hump appeared in the spectra of Si–MNPs and PTA/Si–imid@ Si–MNPs (Fig. 2B and C), at $2\theta = 18–28^{\circ}$, could be assigned to an amorphous silica phase in the shell of $CoFe_2O_4$ nanoparticles. Moreover, there are no characteristic peaks

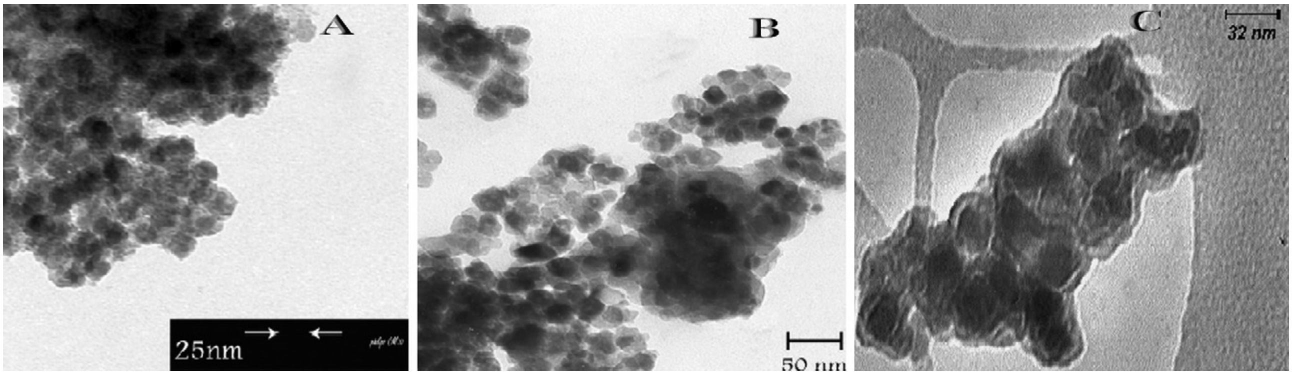

Fig. 3. TEM images of (A) MNPs, (B) Si–MNPs and (C) PTA/Si–imid@ Si–MNPs.

Table 1
Oxidation of alkenes by *t*-BuOOH using PTA/Si–imid@ Si–MNPs catalyst.[a]

Entry	Alkenes	Product	Conversion (%)[b]	Selectivity (%)[b]
1[c]	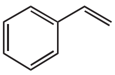	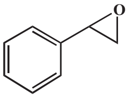	95	90
2[c]	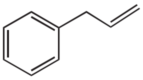	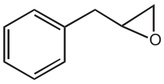	80	90
3[c]	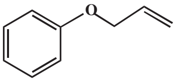	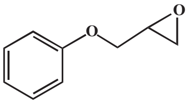	95	92
4[c]		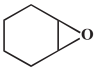	90	95
5[c]	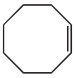	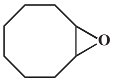	95	95
6[c]		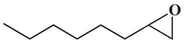	70	95
7[c]		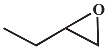	65	90
8[d]	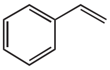	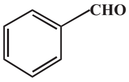	45	80
9[e]	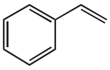	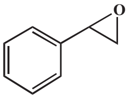	–	–
10[f]	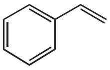	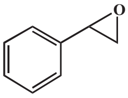	42	65
11[g]	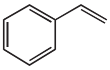	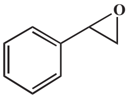	–	–
12[h]	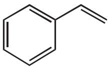	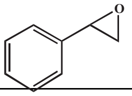	91	90

[a] Reaction conditions: alkene (1 mmol); *t*-BuOOH (2 mmol); catalyst (0.1 g); 1,2-dichloroethane (5 mL); *T*: 70 °C; time: 6 h.
[b] GC yields based on starting alkenes.
[c] Catalyst: PTA/Si–imid@ Si–MNPs.
[d] Catalyst: MNPs.
[e] Catalyst: Si–MNPs.
[f] Catalyst: PTA.
[g] Catalyst: Si–imid@ Si–MNPs.
[h] Fifth recycled catalyst.

of PTA in the XRD spectrum of PTA/Si–imid@ Si–MNPs. This indicates that PTA species are well-dispersed in the surface of the functionalized MNPs and probably there is no crystalline phase of this heteropoly acid to be detected by XRD analysis [43,44].

The TEM images of MNPs, Si–MNPs and PTA/Si–imid@ Si–MNPs are presented in Fig. 3, which reveal that most of the particles have quasi-spherical shape. The average size of these nanoparticles is in the range of 20–30 nm which show a close agreement with the values calculated by XRD analysis. Interestingly, the magnetic core is visible as a dark spot inside the bright spherical SiO_2 thin shell in the TEM images of Si–MNPs and PTA/Si–imid@ Si–MNPs samples (see Fig. 3B and C).

Magnetic measurements for MNPs, Si–MNPs and PTA/Si–imid@ Si–MNPs samples were performed using a vibrating sample magnetometer (VSM) with a peak field of 8 kOe and their hysteresis curves are shown in Fig. 4. It could be seen from the loops in Fig. 4 that saturation magnetization (M_S) of MNPs, Si–MNPs and PTA/Si–imid@ Si–MNPs are 59.42, 38.93 and 21.84 emu/g, respectively. The decrease in mass saturation magnetization in the last two composites is ascribed to the contribution of the

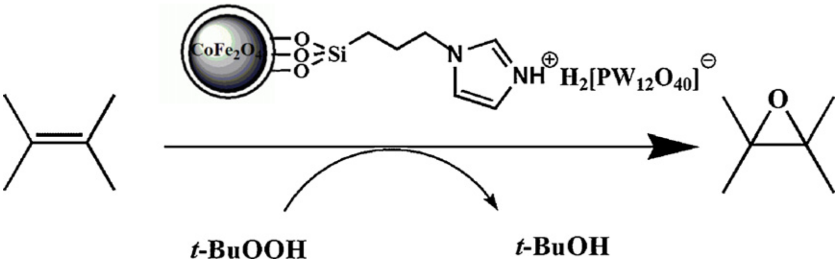

Scheme 2. Oxidation of alkenes using PTA/Si–imid@ Si–MNPs catalyst.

non-magnetic silica shell and functionalized groups. Although the M_S values of the silica coated and functionalized MNPs samples have evidently decreased, they still could be efficiently separated from solution media with a permanent magnet.

There are two weight loss steps in TGA curve of PTA/Si–imid@ Si–MNP catalyst (Fig. 5). The first mass loss of 1.7% (between 60 and 218 °C) may be due to removal of surface adsorbed water of the catalyst. The loss of weight at temperatures higher than 218 °C can be ascribed to the decomposition of Si–imid groups. The TGA analysis of the as-prepared catalyst showed an immidazolium moiety loading of approximately 0.36 mmol/g. Moreover, the tungsten content of the catalyst, as determined by ICP-AES, was 0.98 mmol/g. This is another proof for the fact that PTA was immobilized onto the imidazole functionalized silica coated $CoFe_2O_4$ nanopaticles.

3.2. Oxidation of alkenes

Styrene was examined as a substrate model to optimize reaction conditions using *t*-BuOOH as oxidant in the presence of catalytic amount of PTA/Si–imid@ Si–MNPs. The obtained optimum conditions are: catalyst 0.1 g, oxidant and substrate in a molar ratio of 2:1, respectively. The reaction temperature was set at 70 °C, since a very low conversion of styrene is observed at room temperature. Various solvents, including acetone, chloroform, acetonitrile, and 1,2-dichloroethane were examined to find out the appropriate solvent and 1,2-dichloroethane gave the best results. Besides *t*-BuOOH other oxidants such as H_2O_2 and H_2O_2/urea (UHP) were also screened for the epoxidation of styrene, but *t*-BuOOH was found to be the best source of oxygen. It was also found that no epoxidation reaction of alkenes occurred in the absence of catalyst or oxidant. Moreover, we have also examined bare $CoFe_2O_4$, silica coated $CoFe_2O_4$, neat PTA and Si–imid@ Si–MNPs for the epoxidation of styrene. As it seen in Table 1, bare $CoFe_2O_4$ can oxidize styrene to benzaldehyde with relatively good conversion. However, $CoFe_2O_4$ loses its catalytic activity and becoming inert surface after coating with silica. Also, according to the results of Table 1, neat $H_3PW_{12}O_{40}$ (PTA) shows much lower catalytic activity (42% conversion and 65% selectivity) in the epoxidation reaction of styrene compared with PTA/Si–imid@ Si–MNPs catalyst. Therefore, the high catalytic activity of PTA immobilized on Si–imid@ Si–MNPs catalyst can be attributed to the nanosized character of the support which increases surface area for more interaction with substrates.

The obtained preliminary results for the epoxidation of styrene were encouraging and to extend the scope of this heterogeneous catalytic system, the epoxidation of further olefins was carried out under the optimized conditions (see Scheme 2).

As shown in Table 1, the newly designed PTA based hybrid catalyst can epoxidize styrene, allylbenzene, allyl phenyl ether, cyclohexene and cyclooctene efficiently and selectively in the presence of *t*-BuOOH. Linear alkenes, such as 1-octene and 1-butene were also converted to their corresponding epoxides by PTA/Si–imid@ Si–MNPs with good yields.

3.3. Catalyst recycling

Catalyst reusability is of major importance in heterogeneous catalysis. The recovery and reusability of the catalyst was studied using styrene as model substrate. Catalyst recycling experiments were achieved by fixing the catalyst magnetically at the bottom of the flask and the solution was decanted after each run. The left solid was washed with 1,2-dichloroethane twice, and fresh substrate dissolved in 1,2-dichloroethane is introduced into the flask, allowing the system to proceed for next run. The catalyst was consecutively reused five times without any noticeable loss of its catalytic activity. ICP-AES analysis has shown that leaching of the catalyst from support (1.2% W) occurred only in the first run and no leaching was observed in the next runs. Furthermore, the FT-IR spectrum of the recovered catalyst showed no change after using the catalyst for five successive times. This catalyst has some remarkable features including ease of separation by an external magnet and in contrast to other reported similar catalysts; no regeneration process is required after each reaction [29].

4. Conclusions

In summary, we have successfully developed a novel type of non-covalently immobilized $H_3PW_{12}O_{40}$ catalyst using surface-modified $CoFe_2O_4$ magnetic nanoparticles as support. The as-synthesized catalyst was confirmed by XRD, FT-IR, TGA, TEM, ICP-AES, and VSM techniques. This catalyst was found to epoxidize some alkenes efficiently in the presence of *t*-BuOOH as oxidant. Moreover, the immobilized PTA catalyst could be easily recovered by simple magnetic decantation and reused at least five times without significant loss of activity.

Acknowledgment

The authors wish to acknowledge the support of this work by the Research Council of Shahid Chamran University, Ahvaz, Iran.

References

[1] J.E. Backvall, Modern Oxidation Methods, Wiley–VCH, Weinheim, 2004.
[2] C. Venturello, R.D. Aloisio, J.C. Bart, M. Riai, J. Mol. Catal. A 32 (1985) 107–110.
[3] Y. Ishii, K. Yamawaki, T. Yoshida, T. Ura, H. Yamada, M. Ogawe, J. Org. Chem. 52 (1987) 1868–1870.
[4] Y. Ishii, K. Yamawaki, T. Ura, H. Yamada, T. Yoshida, M. Ogawa, J. Org. Chem. 53 (1988) 3587–3593.
[5] X.M. Yan, J.H. Lei, D. Liu, Y.C. Wu, W. Liu, Mater. Res. Bull. 42 (2007) 1905–1913.
[6] N. Dubey, S.S. Rayalu, N.K. Labhsetwar, S. Devotta, Int. J. Hydrogen Energy 33 (2008) 5958–5966.
[7] M.A. Alibeik, Z. Zaghaghi, I.M. Baltork, J. Chin. Chem. Soc. 55 (2008) 1–4.
[8] K.K. Senapati, C. Borgohain, P. Phukan, J. Mol. Catal. A 339 (2011) 24–31.
[9] J. Tonga, L. Boc, Z. Li, Z. Lei, C. Xia, J. Mol. Catal. A 307 (2009) 58–63.
[10] V. Polshettiwar, R.S. Varma, Tetrahedron (2010) 1091–1097.
[11] M. Ma, Q. Zhang, D. Yina, J. Doua, H. Zhanga, H. Xu, Catal. Commun. 17 (2012) 168–172.
[12] V. Polshettiwar, B. Baruwati, R.S. Varma, Green Chem. 11 (2009) 127–131.
[13] B. Dutta, S. Jana, A. Bhattacharjee, P. Gutlich, S.I. Iijima, S. Koner, Inorg. Chim. Acta 363 (2010) 696–704.
[14] W. Long, C.S. Gill, S. Choi, C.W. Jones, Dalton Trans. 39 (2010) 1470–1472.

[15] V. Polshettiwar, R. Luque, A. Fihri, H. Zhu, M. Bouhrara, J.M. Basset, Chem. Rev. 111 (2011) 3036–3075.
[16] C.W. Lim, I.S. Lee, Nano Today 5 (2010) 412–434.
[17] I.C. Nlebedim, J.E. Snyder, A.J. Moses, D.C. Jiles, J. Magn. Magn. Mater. 322 (2010) 3938–3942.
[18] G.V.M. Jacintho, A.G. Brolo, P. Corio, P.A.Z. Suarez, J.C. Rubim, J. Phys. Chem. C 113 (2009) 7684–7691.
[19] Z.F. Zi, Y. Sun, X. Zhu, Z. Yang, J. Dai, W. Song, J. Magn. Magn. Mater. 321 (2009) 1251–1255.
[20] R.F. Majidi, N.S. Sanjani, F. Agend, Thin Solid Films 515 (2006) 368–374.
[21] L.G. Bach, M.R. Islam, J.T. Kim, S.Y. Seo, K.T. Lim, Appl. Surf. Sci. 258 (2012) 2959–2966.
[22] M. Sheykhana, L. Mamani, A. Ebrahimia, A. Heydari, J. Mol. Catal. A 335 (2011) 253–261.
[23] H. Wang, J. Huang, L. Ding, D. Li, Y. Han, Appl. Surf. Sci. 257 (2011) 7107–7112.
[24] C.S. Gill, B.A. Price, C.W. Jones, J. Catal. 251 (2007) 145–152.
[25] A. Schatz, O. Reiser, W.J. Stark, Chem. Eur. J. 16 (2010) 8959–8967.
[26] X. Peng, Y. Wang, X. Tang, W. Liu, Dyes Pigments 91 (2011) 26–32.
[27] L. Qu, S. Tie, Micropor. Mesopor. Mater. 117 (2009) 402–405.
[28] X. Yan, J. Chen, Q. Xue, P. Miele, Micropor. Mesopor. Mater. 135 (2010) 137–142.
[29] Z. Zhang, F. Zhang, Q. Zhu, W. Zhao, B. Ma, Y. Ding, J. Colloid Interface Sci. 360 (2011) 189–194.
[30] X. Cui, D. Yao, H. Li, J. Yang, D. Hu, J. Hazard. Mater. 205 (2012) 17–23.
[31] X. Zheng, L. Zhang, J. Li, S. Luo, J.P. Cheng, Chem. Commun. 47 (2011) 12325–12327.
[32] J.C. Bailar Jr., Inorg. Synth. 1 (1939) 132–133.
[33] K. Maaz, A. Mumtaz, S.K. Hasanain, A. Ceylan, J. Magn. Magn. Mater. 308 (2007) 289–295.
[34] Y.H. Deng, C.C. Wang, J.H. Hu, W.L. Yang, S.K. Fu, Colloids Surf. A 262 (2005) 87–93.
[35] C.P. Mehnert, J. Chem. Eur. 11 (2005) 50–56.
[36] X. Lang, Z. Li, C. Xia, Synth. Commun. 38 (2008) 1610–1616.
[37] S.X. Ying, W.J. Fa, J. Mol. Catal. A 280 (2008) 142–147.
[38] K. Yamaguchi, C. Yoshida, S. Uchida, N. Mizuno, J. Am. Chem. Soc. 127 (2005) 530–531.
[39] L.T.A. Sofia, A. Krishnan, M. Sankar, N.K. Kala Raj, P. Manikandan, P.R. Rajamohanan, T.G. Ajithkumar, J. Phys. Chem. C 113 (2009) 21114–21122.
[40] M. Ma, Y. Zhang, W. Yu, H.Y. Shen, H. Zhang, N. Gu, Colloids Surf. A 212 (2003) 219–226.
[41] H. Ono, T. Katsumata, Appl. Phys. Lett. 78 (2001) 1832–1834.
[42] T. Rakjumar, G.R. Rao, J. Chem. Sci. 120 (2008) 587–594.
[43] Y. He, C.S. Woo, H.G. Kim, H.I. Lee, Appl. Catal. A 281 (2005) 167–178.
[44] A.G. Siahkali, A. Philippou, J. Dwyer, M.W. Anderson, Appl. Catal. A 192 (2000) 57–69.